Constraining the shell-correction energies of super-heavy nuclei Uncertainty analysis

B. Cauchois, D. Boilley

Constraining the shell-correction energies of super-heavy nuclei

Uncertainty analysis

Bartholomé Cauchois[1,2] and David Boilley[1,2a]

[1] Grand Accélérateur National d'Ions Lourds (GANIL), CEA/DRF - CNRS/IN2P3, BP55027, F14076 Caen Cedex, France
[2] Normandie Université, Unicaen, Caen, France

Abstract. The existence of super-heavy nuclei can only be explained by the introduction of stabilizing ground state shell effects. The macroscopic-microscopic masses are constructed from the sum of a macroscopic, liquid-drop, energy contribution and a microscopic, shell-correction energy. In the present study, shell-correction energies are inferred by subtracting the liquid-drop contributions to their corresponding experimental masses. As most super-heavy nuclei masses are not precisely known, they are deduced from measured Q_α values. Furthermore, a detailed uncertainty analysis regarding experimental masses and more importantly the liquid-drop masses delivers decisive theoretical constraints on shell-correction energies. The current work focuses on two α decay chains, the first, following from a hot fusion reaction leading to the synthesis of ^{291}Lv and the second, following from a cold fusion reaction leading to the synthesis of ^{277}Cn. Contrasting the outcomes obtained for these two decay chains, demonstrates that mass measurement precisions of about 50 keV are required in order to efficiently constrain the shell-correction energies of super-heavy nuclei.

PACS. 21.10.Dr Binding energies and masses – 21.60.Ev Collective Models – 02.50.-r Probability theory, stochastic processes, and statistics – 02.30.Zz Inverse problems
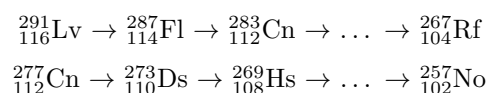
1 Introduction

The existence of super-heavy nuclei (SHN) can only be explained by the introduction of stabilizing ground state shell effects. In addition to ground state properties, shell effects strongly influence the fission barriers which insure the survival of the compound nucleus. Therefore, shell effects play a crucial role in our understanding of both the structure and the production of SHN.

As discussed in ref. [1], shell corrections can be obtained from a broad spectrum of models, however, the results are ultimately dispersed, thus, proving the compelling need to find suitable experimental constraints. Furthermore, these additional quantum effects are included in various ways within the few theoretical approaches, at hand. This leads to discrepancies of few MeV in the fission barriers calculations [2]. In turn, these discrepancies also result in critical changes of the survival probability, and therefore, of the production cross-section of SHN [3].

Given that masses are very sensitive to structural properties, they can provide constraints on shell effects. However, most SHN masses are not precisely known. Nevertheless, assuming that the last mass in an α decay chain is well established, masses can be deduced from measured

Q_α values of decaying nuclei. In particular, we focus our study on the decay chains:

$$^{291}_{116}\text{Lv} \rightarrow {}^{287}_{114}\text{Fl} \rightarrow {}^{283}_{112}\text{Cn} \rightarrow \ldots \rightarrow {}^{267}_{104}\text{Rf}$$

$$^{277}_{112}\text{Cn} \rightarrow {}^{273}_{110}\text{Ds} \rightarrow {}^{269}_{108}\text{Hs} \rightarrow \ldots \rightarrow {}^{257}_{102}\text{No}$$

The first following from a hot fusion reaction and the second from a cold fusion one.

On the grounds that macroscopic-microscopic (MM) models incorporate many structure effects, they certainly provide accurate mass predictions. The MM masses are the sum of a macroscopic liquid-drop (LD) energy contribution and a microscopic shell-correction energy (SCE) contribution which are obtained from single-particle spectra using the Strutinsky method [4,5]. It was shown in ref. [6] with a very simple MM model adjusted to experimental masses that the parameters of the LD are practically uncorrelated to the parameters of the SCE part. This tends to justify the usual MM assumption, i.e., the masses can be expressed as a sum of two distinct contributions. In a similar way, empirical SCE can be inferred by subtracting the LD contribution to the experimental mass. In order to procure consistent results, the LD model should, itself, be fitted using theoretical SCE. From this, it is clear that the empirical SCE deduced from the subtraction of LD contribution to the experimental mass, will depend on both the chosen theoretical SCE and LD model.

---

[a] e-mail: `david.boilley@ganil.fr`

In the following, we repeat the study done in ref. [1] including a detailed uncertainty analysis of the experimental masses and more importantly, of the LD contribution [7]. Considering these uncertainties delivers decisive theoretical constraints on SCE. In addition to the SCE and their uncertainties, we provide correlation matrices for experimental and LD masses, as well as for empirical SCE for all nuclei in the studied decay chains. In order to fully comply with international standards, the formulas needed to compute uncertainties, covariances and correlations were taken from refs. [8,9].

2 Experimental mass excess

Most SHN masses are not precisely known. Nevertheless, assuming the last mass in an α decay chain is known, masses can be deduced from measured Q_α values:

$$\Delta m^{Exp}(A, Z) = \Delta m^{Exp}(A - 4, Z - 2) \\ + Q_\alpha(A, Z) + \Delta_\alpha \quad (1)$$

where $\Delta m^{Exp}(A, Z)$ and $Q_\alpha(A, Z)$ are respectively the mass excess of the mother nucleus and the Q_α value of the α decay. The quantity $\Delta m^{Exp}(A - 4, Z - 2)$ is the mass excess of the daughter nucleus and $\Delta_\alpha = 2.424\,915\,61(6)$ MeV is the α particle's mass excess. In particular, knowing the Q_α values for all nuclei in the decay chain and the mass excess of the last nucleus, here $\Delta m^{Exp}(^{267}\text{Rf})$ or $\Delta m^{Exp}(^{257}\text{No})$, we can deduce all masses within the decay chain. In the present work, it is assumed that the measured Q_α values correspond to transitions from the ground state of the mother nucleus to the ground state of daughter nucleus.

In the following, $\Delta m^{Exp}(^{267}\text{Rf})$, $\Delta m^{Exp}(^{257}\text{No})$ and Δ_α are taken from the AME2016 table [10,11] and the Q_α values were extracted from refs. [12,13]. All of these quantities are given in tables 1 and 2 alongside their uncertainties and are assumed to be uncorrelated as they were measured independently. They appear in italic to indicate that they were not obtained in the present work.

As the quantities entering eq. (1) are uncorrelated, the variance can be estimated using the familiar uncertainty propagation formula:

$$u^2(\Delta m^{Exp}(A, Z)) = u^2(Q_\alpha(A, Z)) + u^2(\Delta_\alpha) \\ + u^2(\Delta m^{Exp}(A - 4, Z - 2)) . (2)$$

In this equation $u(\Delta_\alpha)$ is very small as the alpha particle belongs to the most precisely known masses and thus, plays no role in the present analysis.

Apart from $\Delta m^{Exp}(^{267}\text{Rf})$ and $\Delta m^{Exp}(^{257}\text{No})$, all mass excesses and their uncertainties, shown in tables 1 and 2, were calculated using eqs. (1) and (2), respectively. Clearly, the dominating uncertainty, for the first decay chain, is the one associated with $\Delta m^{Exp}(^{267}\text{Rf})$. However, this is not the case for the second decay chain where the Q_α values uncertainties are the dominating ones.

The calculated mass excesses given in table 1 are compatible with the values given in the AME2016 [11], within

uncertainties that are quite large. This is not the case for the values given in table 2. Note that in the AME2016 table, values and uncertainties were not derived from purely experimental data, but corrected by the trends of the mass surface [10].

From eq. (1), it is clear that the mass of the mother nucleus depends on the mass of the daughter nucleus. Thus, all experimental masses within a decay chain are correlated. The covariance can be easily obtained,

$$u(\Delta m^{Exp}(A, Z), \Delta m^{Exp}(A - 4, Z - 2)) \\ = u^2(\Delta m^{Exp}(A - 4, Z - 2)) . \quad (3)$$

Similarly, all other covariances can be calculated and correlation coefficients can be deduced from these. The results are presented in tables 3 and 4. The correlation matrix for the first decay chain given in table 3 shows strong positive correlations between the experimental masses. This undoubtedly confirms, the influence of the large uncertainty in $\Delta m^{Exp}(^{267}\text{Rf})$ upon all other experimental masses in the decay chain. The outcome for the second decay chain given in table 4 is quite different and shows weak positive correlations between the experimental masses, thus, establishing the limited impact of the small uncertainty in $\Delta m^{Exp}(^{257}\text{No})$ on the experimental masses.

3 LD mass excess

The LD contribution to the mass can be deduced from the binding energy using a specific LD model. In the present work, the LD model was taken from Ref. [14] and is hereby reproduced:

$$B_{LD} = (p_1 + p_2 I^2) A + (p_3 + p_4 I^2) A^{\frac{2}{3}} + p_5 \frac{Z^2}{A^{\frac{1}{3}}} + p_6 \frac{Z^2}{A} \\ + p_7 |N - Z| e^{-\left(\frac{A}{50}\right)^2} + p_8 e^{-80 I^2} + E_{pair}, \quad (4)$$

with $I = (N - Z)/A$. The pairing energy term, E_{pair} in eq. (4), comes from ref. [15] and reads:

$$E_{pair} = \begin{cases} \frac{p_9}{N^{\frac{1}{3}}} + \frac{p_{10}}{Z^{\frac{1}{3}}} + \frac{p_{11}}{A^{\frac{2}{3}}} + \frac{p_{12}}{A} & \text{N=Z, odd} \\ \frac{p_9}{N^{\frac{1}{3}}} + \frac{p_{10}}{Z^{\frac{1}{3}}} + \frac{p_{11}}{A^{\frac{2}{3}}} & \text{N and Z, odd} \\ \frac{p_{10}}{Z^{\frac{1}{3}}} & \text{N even, Z odd} \\ \frac{p_9}{N^{\frac{1}{3}}} & \text{N odd, Z even} \\ 0 & \text{N even, Z even.} \end{cases} \quad (5)$$

As in ref. [14], the LD from eq. (4) is fitted upon experimental masses with added theoretical shell-corrections. The experimental masses were taken from the AME2016 table [10,11] and the theoretical SCE from the Thomas-Fermi model [15,16]. As the sole existence of SHN is based on shell effects, the addition of theoretical SCE to experimental masses is certainly required. However, the stability of SHN cannot be understood by solely looking at the SCE at the ground state. For instance, stability against fission comes from the energy difference between the ground state and the saddle point, i.e., the fission barrier. Nevertheless,

Table 1. Table containing the results concerning the first decay chain along with their uncertainties. The Q_α values and their uncertainties were taken from ref. [12] and $\Delta m^{Exp}(^{267}\text{Rf})$ from refs. [10,11]. The last column gives the theoretical SCE taken from refs. [15,16]. All quantities are given in MeV.

Nuclei	Q_α	Δm^{Exp}	Δm^{LD}	SCE	SCE from refs. [15,16]
$^{267}_{104}\text{Rf}$	-	113.440 ± 0.580	117.140 ± 0.059	-3.700 ± 0.583	-5.08
$^{271}_{106}\text{Sg}$	8.67 ± 0.08	124.535 ± 0.585	128.126 ± 0.063	-3.591 ± 0.589	-5.18
$^{275}_{108}\text{Hs}$	9.44 ± 0.06	136.400 ± 0.589	139.725 ± 0.068	-3.325 ± 0.592	-4.90
$^{279}_{110}\text{Ds}$	9.84 ± 0.06	148.665 ± 0.592	151.929 ± 0.074	-3.264 ± 0.596	-4.91
$^{283}_{112}\text{Cn}$	9.67 ± 0.06	160.760 ± 0.595	164.731 ± 0.081	-3.971 ± 0.600	-6.19
$^{287}_{114}\text{Fl}$	10.16 ± 0.06	173.345 ± 0.598	178.124 ± 0.090	-4.779 ± 0.604	-7.74
$^{291}_{116}\text{Lv}$	10.89 ± 0.07	186.659 ± 0.602	192.101 ± 0.099	-5.442 ± 0.610	-8.07

Table 2. Table containing the results concerning the second decay chain along with their uncertainties. The Q_α values and their uncertainties were deduced from the α particle's energies presented in ref. [13] and $\Delta m^{Exp}(^{257}\text{No})$ from refs. [10,11]. The last column gives the theoretical SCE taken from refs. [15,16]. All quantities are given in MeV.

Nuclei	Q_α	Δm^{Exp}	Δm^{LD}	SCE	SCE from refs. [15,16]
$^{257}_{102}\text{No}$	-	90.247 ± 0.007	94.833 ± 0.049	-4.586 ± 0.050	-5.77
$^{261}_{104}\text{Rf}$	8.65 ± 0.02	101.322 ± 0.021	106.075 ± 0.054	-4.753 ± 0.058	-6.79
$^{265}_{106}\text{Sg}$	8.84 ± 0.03	112.587 ± 0.037	117.918 ± 0.061	-5.331 ± 0.071	-6.38
$^{269}_{108}\text{Hs}$	9.35 ± 0.02	124.362 ± 0.042	130.357 ± 0.068	-5.995 ± 0.080	-5.30
$^{273}_{110}\text{Ds}$	11.31 ± 0.02	138.097 ± 0.046	143.383 ± 0.076	-5.286 ± 0.089	-4.34
$^{277}_{112}\text{Cn}$	11.42 ± 0.02	151.942 ± 0.050	156.991 ± 0.085	-5.049 ± 0.099	-4.11

Table 3. Experimental mass excess correlation matrix for the first decay chain.

^{267}Rf	1.00	0.99	0.98	0.98	0.97	0.97	0.96
^{271}Sg	0.99	1.00	0.99	0.98	0.98	0.97	0.97
^{275}Hs	0.98	0.99	1.00	0.99	0.98	0.98	0.97
^{279}Ds	0.98	0.98	0.99	1.00	0.99	0.98	0.98
^{283}Cn	0.97	0.98	0.98	0.99	1.00	0.99	0.98
^{287}Fl	0.97	0.97	0.98	0.98	0.99	1.00	0.99
^{291}Lv	0.96	0.97	0.97	0.98	0.98	0.99	1.00

Table 4. Experimental mass excess correlation matrix for the second decay chain.

^{257}No	1.00	0.33	0.19	0.16	0.15	0.13
^{261}Rf	0.33	1.00	0.57	0.50	0.45	0.41
^{265}Sg	0.19	0.57	1.00	0.87	0.79	0.72
^{269}Hs	0.16	0.50	0.87	1.00	0.90	0.82
^{273}Ds	0.15	0.45	0.79	0.90	1.00	0.91
^{277}Cn	0.13	0.41	0.72	0.82	0.91	1.00

in the following we shall only focus our attention on the SCE at the ground state.

The uncertainty in the parameters is estimated with the standard regression analysis method which stands on an extended mathematical corpus. The main features are recalled here for the sake of completeness. The errors of the model ϵ are added in order to encompass its shortcomings and it is assumed that the experimental masses can be described by

$$\Delta m^{Exp} = \Delta m^{LD} + SCE + \epsilon. \qquad (6)$$

As usual in standard regression, it is also assumed that the errors follow a Gaussian distribution with zero mean and a uniform variance σ (homoscedastic hypothesis). As detailed in ref. [7], these errors leads to uncertainties in the parameters of the LD model and in all deduced quantities. In this article, we use the vocabulary of the GUM [8] that distinguishes errors defined as deviations of the model from the "true" experimental data, and the uncertainties that estimate the dispersion of a quantity. It should be borne in mind that the model is only meant to describe the LD energies, while the errors may also inherit flaws from the liquid-drop itself including pairing, the shell corrections, as well as other issues having unknown origins.

Note that the uncertainties in the experimental binding energies were neglected as they are very small with respect to the errors, and uncertainties in the theoreti-

Table 5. Theoretical LD mass excess correlation matrix for the first decay chain.

^{267}Rf	1.00	0.99	0.97	0.94	0.91	0.88	0.84
^{271}Sg	0.99	1.00	0.99	0.97	0.95	0.93	0.90
^{275}Hs	0.97	0.99	1.00	0.99	0.98	0.96	0.94
^{279}Ds	0.94	0.97	0.99	1.00	0.99	0.98	0.97
^{283}Cn	0.91	0.95	0.98	0.99	1.00	0.99	0.99
^{287}Fl	0.88	0.93	0.96	0.98	0.99	1.00	0.99
^{291}Lv	0.84	0.90	0.94	0.97	0.99	0.99	1.00

Table 7. SCE correlation matrix for the first decay chain.

^{267}Rf	1.00	0.99	0.98	0.97	0.97	0.96	0.96
^{271}Sg	0.99	1.00	0.99	0.98	0.98	0.97	0.97
^{275}Hs	0.98	0.99	1.00	0.99	0.98	0.98	0.97
^{279}Ds	0.97	0.98	0.99	1.00	0.99	0.98	0.98
^{283}Cn	0.97	0.98	0.98	0.99	1.00	0.99	0.98
^{287}Fl	0.96	0.97	0.98	0.98	0.99	1.00	0.99
^{291}Lv	0.96	0.97	0.97	0.98	0.98	0.99	1.00

Table 6. Theoretical LD mass excess correlation matrix for the second decay chain.

^{257}No	1.00	0.99	0.97	0.95	0.92	0.90
^{261}Rf	0.99	1.00	0.99	0.98	0.96	0.94
^{265}Sg	0.97	0.99	1.00	0.99	0.98	0.97
^{269}Hs	0.95	0.98	0.99	1.00	0.99	0.99
^{273}Ds	0.92	0.96	0.98	0.99	1.00	0.99
^{277}Cn	0.90	0.94	0.97	0.99	0.99	1.00

cal shell correction energies are disregarded at this stage because they are not available.

In this study, the parameters, their uncertainties and correlation matrix, obtained as in ref. [7], are reported in appendix A. The LD contributions to the masses of the nuclei entering an α decay chain, are established with the same formula and parameters, consequently, they are very strongly correlated. Results, for the two decay chains, are presented in tables 1 and 2 while the corresponding correlation matrices are exposed in tables 5 and 6, respectively.

Note that the uncertainties in the LD masses are very small with respect to the errors of the model, estimated by the root mean square of the fit: $\hat{\sigma} = RMS = 602$ keV.

4 Deduced empirical shell-correction energies

In sect. 2, informations regarding the α decay chains were used to determine Δm^{Exp} and in sect. 3, a specific LD model was used to obtain Δm^{LD}. As mentioned in the introduction, empirical SCE of can be inferred by subtracting the LD contribution to the experimental masses:

$$SCE = \Delta m^{Exp} - \Delta m^{LD}. \qquad (7)$$

Notice, the two terms entering the r.h.s. of eq. (7) are independent, thus, SCE uncertainties simply read:

$$u^2\left(SCE\right) = u^2\left(\Delta m^{Exp}\right) + u^2\left(\Delta m^{LD}\right). \qquad (8)$$

The SCE are given side by side with their uncertainties in tables 1 and 2 and contrasting these tables yields the ensuing conclusion. Since, the last masses in decay chains, following from hot fusion reactions, are not precisely known,

the corresponding SCE are loosely constrained and certainly, one could assert the opposite for decay chains subsequent to cold fusion reactions. Nevertheless, climbing-up the decay chain, the uncertainties in the SCE tend to grow, reaching their maximum for the mother nucleus. This is a direct consequence of the increasing number of Q_α values involved, along with their uncertainties, and causing the escalation of uncertainties in the SCE.

If we include the error of the model into the analysis, the previous equation becomes

$$u^2\left(SCE\right) = u^2\left(\Delta m^{Exp}\right) + u^2\left(\Delta m^{LD}\right) + \hat{\sigma}^2. \qquad (9)$$

Typical values range from 604 et 610 keV for the second chain given in table 2. This shows that errors are dominating in this case. Regarding the first decay chain given in table 1, uncertainties in the experimental masses are similar to the standard deviation of the errors and typical values for uncertainties in SCE including errors range from 838 to 857 keV.

As discussed in sect. 2, the values taken by Δm^{Exp} all are correlated together. Likewise, in sect. 3, we have seen that all Δm^{LD} are correlated together. Accordingly, this is also the case for SCE of all nuclei in a decay chain. As for the experimental and LD masses, we can construct the SCE correlation matrices given in tables 7 and 8. Notice, in the case of the first decay chain that the correlations regarding experimental masses, cf. table 3, and those concerning SCE, cf. table 7, are very resemblant. This can be interpreted as coming from the uncertainty in $\Delta m^{Exp}(^{267}\text{Rf})$ which plainly prevails over all other sources of both uncertainties and correlations. However, in the case of the second decay chain, tables 4 and 8 do not share this similarity. This can be understood as coming from the minute uncertainty associated with $\Delta m^{Exp}(^{257}\text{No})$. Consequently, the SCE correlations may only be explained by the strong correlations between LD masses.

5 Discussion and conclusion

Masses and shell correction energies are very sensitive parameters of the estimate of super-heavy production cross-sections as they affect the Q-value of the reaction and the fission barrriers [3]. Thus, their uncertainties as well as their covariances should be carefully estimated before estimating uncertainties in these cross-sections or adjusting the other parameters of the underlying models.

Table 8. SCE correlation matrix for the second decay chain.

^{257}No	1.00	0.93	0.83	0.81	0.79	0.77
^{261}Rf	0.93	1.00	0.90	0.87	0.85	0.83
^{265}Sg	0.83	0.90	1.00	0.96	0.93	0.90
^{269}Hs	0.81	0.87	0.96	1.00	0.97	0.94
^{273}Ds	0.79	0.85	0.93	0.97	1.00	0.97
^{277}Cn	0.77	0.83	0.90	0.94	0.97	1.00

In MM models, the SCE is generally determined from single particle spectra. To ensure the consistency of the whole mass description, another adjustment is necessary to guarantee that $\Delta m^{Exp} = \Delta m^{LD} + SCE$. In order to assess the consistency between the microscopic and macroscopic contributions of existing microscopic-macroscopic models, we propose, in the present work to infer empirical SCE by subtracting the LD contributions to their corresponding experimental masses. Assuming the last masses entering the decay chains were known, experimental masses were deduced from measured Q_α values, together with their uncertainties. The LD contributions to the masses were calculated using a specific LD model which was fitted to experimental masses, corrected by theoretical SCE. The uncertainty analysis of the LD part of the mass is based on standard regression that accounts for the errors of the complete MM model even if the uncertainties in theoretical SCE were not included because they are not available. The present work is a first step toward a more extended uncertainty analysis of a complete MM model.

Excluding the correlation matrices, all the results gathered in this work are presented in tables 1 and 2. Efforts were made to provide uncertainties for every calculated quantity within the present work. Considering these uncertainties brings theoretical constrains on SCE which play a crucial role in our understanding of both the structure and the production of SHN.

As some of the SHN masses, e.g., $\Delta m^{Exp}(^{267}$Rf$)$, bear considerable uncertainties which plainly prevail over all other sources of both uncertainties and correlations. This study confirms that improved SHN mass measurements are absolutely necessary in order to better constrain SCE. Following up on this idea, reducing the mass uncertainty of the last nucleus in a decay chain to about 50 keV should be enough and any further reduction would be fruitless as the dominating uncertainties would then be coming from measured Q_α values and the LDM.

One should be cautious as it should be stressed that MM masses are obtained by minimizing the total sum of the LD energy and the theoretical SCE with respect to deformation. Thus, both the macroscopic and microscopic parts of the MM model are coherently glued together through deformation. As the chosen LD model bears no deformation and the theoretical SCE were obtained independently, this coherence is lost in the present study. Once again, it is clear that the SCE deduced in the present work depend on both the chosen theoretical SCE and LD model.

A Liquid drop model

In this appendix, we present the results relative to the regression analysis of the liquid-drop model used in this work, cf. eq. (4).

The model is adjusted to the nuclear binding energies deduced from the atomic mass excesses found in refs. [10, 11] for all nuclei satisfying N,Z $\geq$ 8 with uncertainties below 150 keV, thus, a total of 2315 nuclei are considered.

As discussed in ref. [7], the uncertainties in the parameters and the correlations between them, are a direct consequence of the regression hypotheses. According to these hypotheses, the errors follow a gaussian distribution with zero mean and variance σ^2. This variance can then be propagated onto the parameters leading to their covariances, from which, their uncertainties and correlations can be deduced.

Table 9 contains the parameters and their uncertainties while table 10 presents the correlations between the parameters. The detailed regression analysis is fully exposed in ref. [7]. However, in the present work, the pairing, cf. eq. (5), is adjusted as well which was not done in ref. [7]. Nevertheless, the method remains unchanged.

References

1. S. Hofmann et al., Eur. Phys. J. A **52**, 116 (2016).
2. A. Baran, M. Kowal, P. -G. Reinhard, L. M. Robledo, A. Staszczak, M. Warda, Nucl. Phys. A **944**, 442 (2015)
3. H. Lü, D. Boilley, Y. Abe, C. Shen, Phys. Rev. C **94**, 034616 (2016)
4. V. M. Strutinsky, Nucl. Phys. A **95**, 420 (1967).
5. V. M. Strutinsky, Nucl. Phys. A **122**, 1 (1968).
6. B. Cauchois, PhD thesis, Université de Caen Normandie Université (2018)
7. B. Cauchois, H. Lü, D. Boilley, G. Royer, Phys. Rev. C **98**, 024305 (2018)
8. BIPM, IEC, IFCC, ILAC, ISO, IUPAC, *GUM 1995 with minor corrections. Evaluation of measurement data - Guide to the expression of uncertainty in measurement* (2008)
9. L. Kirkup, B. Frenkel, *An Introduction to Uncertainty in Measurements: Using the GUM* (Cambridge University Press, New-York, 2006)
10. W. J. Huang, G. Audi, M. Wang, F. G. Kondev, S. Naimi, X. Xu, Chin. Phys. C **41** (2017) 030002
11. M. Wang, G. Audi, F. G. Kondev, W. J. Huang, S. Naimi, X. Xu, Chin. Phys. C **41** (2017) 030003
12. Yu. Ts. Oganessian, J. Phys. G: Nucl. Part. Phys. **34**, R165 (2007).
13. K. Morita, J. Phys. Soc. Jpn. **73** (2007) 043201
14. G. Royer, A. Subercaze, Nucl. Phys. A **917**, 1 (2013)
15. W. D. Myers, W. J. Swiatecki, Nucl. Phys. A **601**, 141 (1996)
16. W. D. Myers, W. J. Swiatecki, LBL report 36803 (1994)

Table 9. LDM Parameters and uncertainties in MeV [7]. Here $RMS = 0.602$ MeV.

	p_1	p_2	p_3	p_4	p_5	p_6	p_7	p_8	p_9	p_{10}	p_{11}	p_{12}
Parameters	15.4841	-27.8539	-17.5768	31.2893	-0.7056	0.9107	-0.3071	2.8128	-4.75	-4.68	6.63	12.89
Uncertainties	0.0145	0.0850	0.0507	0.3824	0.0008	0.0294	0.0296	0.1726	0.13	0.12	1.00	6.04

Table 10. LDM Parameters correlation matrix [7].

p_1	p_2	p_3	p_4	p_5	p_6	p_7	p_8	p_9	p_{10}	p_{11}	p_{12}
1.00	-0.71	-0.92	0.47	-0.87	-0.31	0.73	0.80	0.04	0.03	-0.03	-0.02
-0.71	1.00	0.61	-0.92	0.37	0.52	-0.22	-0.87	-0.03	-0.02	0.01	0.12
-0.92	0.61	1.00	-0.48	0.95	-0.06	-0.80	-0.67	-0.08	-0.07	0.05	-0.04
0.47	-0.92	-0.48	1.00	-0.21	-0.26	0.05	0.72	0.03	0.03	-0.01	-0.12
-0.87	0.37	0.95	-0.21	1.00	-0.17	-0.85	-0.48	-0.04	-0.02	0.03	-0.09
-0.31	0.52	-0.06	-0.26	-0.17	1.00	0.16	-0.57	0.05	0.04	-0.02	0.19
0.73	-0.22	-0.80	0.05	-0.85	0.16	1.00	0.37	-0.03	-0.05	-0.01	0.13
0.80	-0.87	-0.67	0.72	-0.48	-0.57	0.37	1.00	-0.03	-0.03	0.02	-0.19
0.04	-0.03	-0.08	0.03	-0.04	0.05	-0.03	-0.03	1.00	0.45	-0.66	0.06
0.03	-0.02	-0.07	0.03	-0.02	0.04	-0.05	-0.03	0.45	1.00	-0.67	0.07
-0.03	0.01	0.05	-0.01	0.03	-0.02	-0.01	0.02	-0.66	-0.67	1.00	-0.24
-0.02	0.12	-0.04	-0.12	-0.09	0.19	0.13	-0.19	0.06	0.07	-0.24	1.00